Assessment of Vibrotactile Feedback on Postural Stability During Pseudorandom Multidirectional Platform Motion

Kathleen H. Sienko*, Vivek V. Vichare, M. David Balkwill, and Conrad Wall, III, *Member, IEEE*

***Abstract*—This study uses frequency-domain techniques and stabilogram diffusion analysis (SDA) to investigate the effect of vibrotactile feedback during continuous multidirectional perturbations of a support platform. Eight subjects with vestibular deficits were subjected to two-axis pseudorandom surface platform motion while donning a multiaxis vibrotactile feedback device that mapped body tilt estimates onto their torsos via a 3-row by 16-column array of tactile vibrators (tactors). Four tactor display configurations with spatial resolutions ranging between 22.5° and 90°, in addition to the tactors OFF configuration, were evaluated. Power spectral density functions of body sway in the anterior–posterior (A/P) and medial–lateral (M/L) directions, and transfer functions between platform motion and body sway, were computed at frequencies ranging from 0.0178 to 3.56 Hz. Cross-spectral analysis revealed that the A/P responses were not significantly driven by M/L inputs, and vice versa, thus supporting the notion of independent A/P and M/L postural control. Vibrotactile feedback significantly decreased A/P and M/L spectral power, decreased transfer function gains up to a frequency of 1.8 and 0.6 Hz in the A/P and M/L directions, respectively, and increased phase leads above 0.3 Hz. SDA showed significantly decreased transition time for both A/P and M/L tilts, and decreased transition displacement and short-term diffusion coefficients for A/P tilt. However, the spatial resolution of the tactor displays did not affect subjects' performance, thereby supporting the use of a lower spatial resolution display in future device designs.**

***Index Terms*—Balance, balance aid, frequency-domain analysis, postural control, stabilogram diffusion analysis (SDA), vibrotactile display.**

I. Introduction

HUMAN postural dynamics are inherently unstable and require complex control mechanisms in order to maintain upright balance. Visual, vestibular, and proprioceptive information are continuously sampled, processed, and integrated by the central nervous system in order to generate corrective motor torques at the feet against the support surface. Individuals with vestibular and proprioceptive loss (i.e., peripheral neuropathy) often experience increased difficulty in maintaining their balance in the absence of visual cues, in poorly lighted environments, or when proprioceptive cues are distorted (i.e., soft, uneven ground) [1].

Sensory substitution is a technique of replacing or augmenting compromised sensory information. Balance aids using various modes of sensory substitution such as electrotactile, vibrotactile, and auditory feedback of body motion have been developed and found effective in improving postural stability of subjects with vestibular loss during stationary tasks and during single-axis perturbed stance [2]–[6]. Sienko *et al.* [7] recently demonstrated that subjects with vestibular loss donning a multiaxis vibrotactile feedback balance aid during continuous multidirectional surface perturbations: 1) reduced their root-mean-square (RMS) trunk sway; 2) decreased their trunk trajectory area; and 3) spent more time in maintaining a near upright posture (as per instructions), when feedback was provided.

Human bipedal quiet stance is most simply modeled by an inverted pendulum [8], [9] with sensory information being combined linearly [10], [11] and controlled by two orthogonal feedback controllers [12] in the anterior–posterior (A/P) and medial–lateral (M/L) directions. Given that the corrective motor torques are generated at the ankle, resulting in negligible knee or hip moments, the use of a simple linearized model to approximate the nonlinear system dynamics is appropriate in the case of quiet stance. While impulse and step functions are effective signals for testing linear systems, it is difficult to find naturally occurring signals that approximate these highly idealized waveforms [13]. Instead, continuously varying support surface stimuli (pseudorandom time series) may be used to study system dynamics by producing steady-state postural responses from which transfer functions can be derived [14].

Power spectral density (PSD) analysis describes the distribution of power content across frequencies for a signal or time series [15]. In the context of human postural control, PSD analysis is used to determine the spectral power content and dominant frequency of body sway during quiet and perturbed stances. A transfer function, defined as the mathematical relationship between the output and input for a linear time-invariant system, characterizes system dynamics with a gain and phase at each frequency. Peterka and Wall used this approach to quantify the effectiveness of a vibrotactile balance aid during single-axis perturbations [16]. In this study, we extend the analysis to assess the utility of a vibrotactile balance aid during multidirectional continuous surface perturbations. In particular, this paper applies techniques such as PSD analysis and frequency transfer

Manuscript received June 26, 2009; revised September 22, 2009. First published November 20, 2009; current version published March 24, 2010. This work was supported by the National Institutes of Health (National Institute on Deafness and Other Communication Disorders R01 DC6201). *Asterisk indicates corresponding author.*

*K. H. Sienko is with the Department of Mechanical Engineering, University of Michigan, Ann Arbor, MI 48109 USA (e-mail: sienko@umich.edu).

V. V. Vichare is with the Department of Mechanical Engineering, University of Michigan, Ann Arbor, MI 48109 USA (e-mail: vvichare@umich.edu).

M. D. Balkwill and C. Wall, III are with the Department of Otology and Laryngology, Harvard Medical School, Massachusetts Eye and Ear Infirmary, Boston, MA 02114 USA (e-mail: dbalkwill@meei.harvard.edu; cwall@mit.edu).

Digital Object Identifier 10.1109/TBME.2009.2036833

function analysis to gain quantitative insight into the frequency-dependent effects of vibrotactile feedback during continuous multidirectional surface perturbations, including possible cross-axis effects that would be indicative of dependent strategies, as opposed to independent strategies for A/P and M/L postural control. A preliminary version of this paper has appeared in [17].

Stabilogram diffusion analysis (SDA) treats postural sway as a stochastic process similar to a random walk [18]. Mean-square displacement of the postural sway is calculated as a function of time interval resulting in two distinct displacement regions. For short time intervals (typically $<$0.5 s), the mean-square displacement is positively correlated and indicates passive open-loop control, whereas for long time intervals (typically $>$1 s), it is negatively correlated and indicates active closed-loop control. SDA parameters provide a further basis on which to quantify the effects of the balance aid.

Fig. 1. Vibrotactile feedback balance aid.

II. Methods

A. Subjects

Eight weakly compensated vestibulopathic subjects (51 $\pm$ 10 years) were referred by the Massachusetts Eye and Ear Infirmary (MEEI) Department of Otolaryngology clinicians for this study (details described in [7]). Weakly compensated subjects were defined as those subjects who failed the NeuroCom Equi-Test computerized dynamic posturography sensory organization tests (SOTs) 5 and 6. During SOT 5, the subject's eyes are closed and the posture platform is sway-referenced (i.e., moves in synchrony with the subject's A/P body sway). SOT 6 is performed with the subject's eyes open, while both the platform and visual surround are sway-referenced. Subjects with histories of mental illness or motor deficits were excluded. Additionally, individuals with a body mass index greater than 30 were excluded due to the size constraints of the vibrotactile balance aid. Subjects gave their informed consent prior to the start of the experiment. The experimental protocol, which conformed to the Helsinki Declaration, was approved by the MEEI, Boston University, and Massachusetts Institute of Technology Institutional Review Boards.

B. Equipment and Instrumentation

Subjects stood on a custom-built 2.1 m by 2.1 m BALance DisturbER (BALDER) platform [19] that could independently move in two orthogonal directions (x and y directions) in an earth horizontal plane. Two-axis platform position data were collected after digitization at 100 Hz.

The vibrotactile balance aid (see Fig. 1) consisted of a two-axis inertial measurement unit (IMU) mounted on the lower back of the subject to capture the trunk dynamics, a vibrotactile array worn around the trunk to intuitively display body motion, and a laptop with analog and digital interfaces. The trunk tilt estimates in the A/P and M/L directions, which aligned with the platform in the y and x directions, respectively, were obtained by processing the IMU's accelerometer and gyroscope measurements. The tilt estimates were displayed on a 3-row by 16-column vibrotactile array worn about the subjects' trunk; the rows displayed estimated tilt magnitude and the columns displayed tilt direction.

The tilt signal presented to the wearer was a combination of tilt angle and half the tilt rate. Three tactor display configurations (4, 8, and 16) evaluated the effects of spatial resolution by varying the number of active tactor columns: the 4-column display used only the tactors in the four cardinal directions, the 8-column display used every second column, and the 16-column display used all columns. The direction of tilt (azimuth) was calculated from the arctangent of the A/P and the M/L components, which in turn activated the appropriate tactor column using the "nearest neighbor" principle. Depending on the direction of the tilt in these three configurations, a single tactor was activated when the tilt angle plus half the tilt rate exceeded a threshold of 1°, while no feedback was given within this threshold. One out of the eight subjects used a 0.5° threshold. A fourth configuration (4I) was treated as two separate single-axis systems, thus displaying A/P tilt and M/L tilt information independent of each other.

C. Platform Stimuli

The support surface was driven by a velocity (v) command sequence created from a 624-length (maximal) pseudorandom pentary sequence (PRPS). Fixed values of $+2v$, $+\ v$, 0, $-\ v$, and $-2v$ were assigned to a four-stage, modulo 5 addition shift-register output with a state duration of $\Delta t = 0.09$ s (see Fig. 2). The resultant sequence had a duration of 56.16 s and a magnitude proportional to the desired platform velocity. This sequence was low-pass filtered (fourth-order Butterworth, cutoff frequency $f_c = 3$ Hz) and integrated to create the position waveform. The initial value of the shift register was selected such that the position waveform was balanced between negative and positive values over one stimulus cycle. The x- and y-platform velocity command signals were given by two uncorrelated waveforms and scaled, so that the RMS velocity of platform motion ranged from 2.4 to 4.2 cm/s. A 3-min stimulus for the testing trials was generated by concatenating three repetitions of a separate pair of waveforms, plus an additional 15 s of the same waveforms to allow the postural control system to reach steady state. The

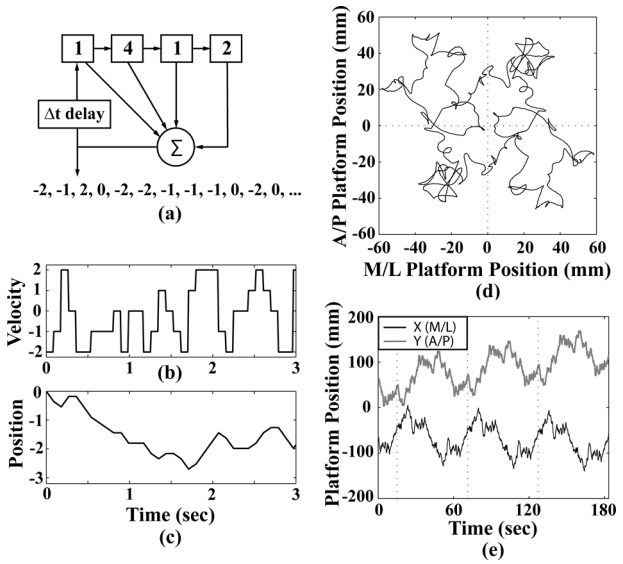

Fig. 2. (a) Modulo 5 shift register. (b) Time series proportional to desired platform velocity. (c) Integrated time series proportional to position. (d) Bird's eye view of one cycle of actual platform position. (e) X- and Y-platform position showing the initial 15 s followed by the three repetitions of the PRPS waveforms, with plots offset for display purposes.

initial 15 s of each trial were not included in the later analysis. The magnitude of the stimulus was adjusted during the training session based on each subject's subjective balance capabilities. Subjects were asked to rate how difficult it was to maintain their balance on a scale of 1 to 10 with 1 and 10 corresponding to not challenging and most difficult balance challenge to date, respectively. The magnitude of the stimulus was adjusted until subjects reported a score of either 6 or 7.

D. Experimental Protocol

The subject was presented with four tactor display configurations, the order of which was varied according to a balanced Latin-squares design [20] with tactor configuration as the primary factor.

This design produced four groups with two subjects in each group. All subjects were given a core test battery of six trials: first, a trial with tactors Off (OFF1), followed by trials with the four tactor configurations, and finally, a second trial with tactors Off (OFF2). The present analysis is based on these six core trials.

Subjects were not told about which tactor configuration they were using unless the tactors were OFF. Subjects were instructed to close their eyes for all trials and move in such a manner so as to null any vibrations regardless of the display configuration. Their feet were positioned hip-width apart and skewed slightly outward on the BALDER force plate.

III. Frequency-Domain Analysis

Frequency-domain analyses were performed by computing PSD functions of body sway measures (trunk tilt in the A/P and the M/L directions) and platform velocity, as well as transfer function and coherence function estimates relating the stimulus (platform motion) and response (trunk tilt).

PSD functions were computed using a discrete Fourier transform (DFT) to decompose the PRPS stimulus and response signals into sinusoidal components [15]. The DFT was applied to each 56.16 s (624 × 0.09 s) cycle of each trial's stimulus and response waveforms. The DFT was calculated at 200 frequencies ranging from $f = 1/56.16 = 0.0178$ to $f = 200/56.16 = 3.56$ Hz. The even frequency points, which have almost zero amplitude, were discarded, thus leaving 100 frequency samples. The PSD functions for the stimulus $G_x(\omega)$ and response $G_y(\omega)$ were averaged over the three cycles for each trial as follows:

$$G_x(\omega) = \frac{1}{3}\sum_{i=1}^{3} X_i(j\omega)^* X_i(j\omega) \tag{1}$$

$$G_y(\omega) = \frac{1}{3}\sum_{i=1}^{3} Y_i(j\omega)^* Y_i(j\omega) \tag{2}$$

where $X_i(j\omega)$ and $Y_i(j\omega)$ are the DFTs of the ith stimulus (platform velocity) and response (trunk tilt) cycles, respectively, $\omega = 2\pi f$, * indicates a complex conjugate, and f is the frequency in hertz. Similarly, the cross PSD function between the stimulus and the response is given by

$$G_{xy}(j\omega) = \frac{1}{3}\sum_{i=1}^{3} X_i(j\omega)^* Y_i(j\omega). \tag{3}$$

The smoothed PSD and cross PSD functions $G_{xs}(\omega)$, $G_{ys}(\omega)$, and $G_{xys}(j\omega)$ were computed using (4)–(6) by averaging adjacent frequency points into 17 frequency bins, such that the number of points averaged increased with the frequency

$$G_{xs}(\omega) = \frac{1}{n}\sum_{i=1}^{n} G_x(\omega) \tag{4}$$

$$G_{ys}(\omega) = \frac{1}{n}\sum_{i=1}^{n} G_y(\omega) \tag{5}$$

$$G_{xys}(j\omega) = \frac{1}{n}\sum_{i=1}^{n} G_{xy}(j\omega) \tag{6}$$

where n is the number of frequency points in each bin.

The PSD function of the PRPS stimulus has equal power contained across all frequencies up to a cutoff frequency. The mean power frequencies (7) and median power frequencies were determined for the computed PSDs as well. The mean frequency of a power spectrum is defined as the normalized, one-sided, first-order spectral moment, whereas the median frequency is defined as the particular frequency that would divide the power spectrum into two parts of equal area as follows:

$$\text{Mean Power Frequency} = \frac{\int \omega P(\omega)\, d\omega}{\int P(\omega)\, d\omega} \tag{7}$$

where ω is the frequency in radians per second and $P(\omega)$ is the PSD function computed at that frequency.

Frequency transfer functions and coherence estimates were computed from the spectra, as described in [15]. The complex transfer functions $H_s(j\omega)$ in (8) were estimated from the PSD and cross PSD functions, and the gain and the phase of the transfer function were subsequently computed using

$$H_s(j\omega) = \frac{G_{xys}(j\omega)}{G_{xs}(j\omega)} \tag{8}$$

$$|H_s(\omega)| = \sqrt{H_s(j\omega)^* H_s(j\omega)} \tag{9}$$

$$\text{phase}(H_s(j\omega)) = \frac{180^\circ}{\pi} \tan^{-1}\left(\frac{\text{Im}(H_s(j\omega))}{\text{Re}(H_s(j\omega))}\right). \tag{10}$$

The phase was computed using MATLAB function "phase." This function "unwraps" the phase values, which means that phase values more negative than 180° could be obtained in cases where phase lags were increasing with increasing frequency. The coherence function estimate $\gamma^2(\omega)$ was computed as follows:

$$\gamma^2(\omega) = \frac{|G_{xys}(\omega)|^2}{G_{xs}(\omega)^* G_{ys}(\omega)}. \tag{11}$$

Coherence function estimates show the degree of correlation between the response and the stimulus as a function of frequency with values ranging from 0 to 1. A value of 1 implies a perfect linear relationship between the stimulus and response and no noise in the system or measurements. The coherence function in the frequency domain is analogous to the cross correlation function in the time domain. 95% confidence intervals for the transfer functions using coherence function estimates were computed, as described in [21].

IV. Stabilogram Diffusion Analysis

Stabilogram diffusion functions (SDFs) were calculated for each cycle in terms of the mean-square displacement for M/L tilt (Δx^2), A/P tilt (Δy^2), and planar tilt ($\Delta r^2 = \Delta x^2 + \Delta y^2$) as a function of time interval (Δt), which ranged from 0.01 to 10 s. The six cycles for OFF1 and OFF2 were grouped and the five most consistent SDFs were averaged to produce a mean SDF for each subject in the tactors OFF condition. Similarly, the four tactor configurations were averaged, retaining 10 of 12 cycles, to produce a mean SDF for the tactors ON condition.

The mean SDF was plotted on both linear and logarithmic scales (see Fig. 3). The first point at which the slope of the log–log plot dropped below 1 was classified as the "transition point," yielding transition time T_t and transition displacement R_t, dividing the plot into short- and long-term regions. Best-fit lines (minimal mean-square error) were determined for the short- and long-term regions, and one-half of their slopes were calculated as the scaling exponents H_s and H_l. Best-fit lines were also determined in the linear domain and one-half of their slopes were calculated as the diffusion coefficients D_s and D_l; the intersection of these lines produced the "critical point" coordinates of critical time T_c and critical displacement R_c. Transition and critical points differ from, but are highly correlated with each other; both have been reported in the literature [18].

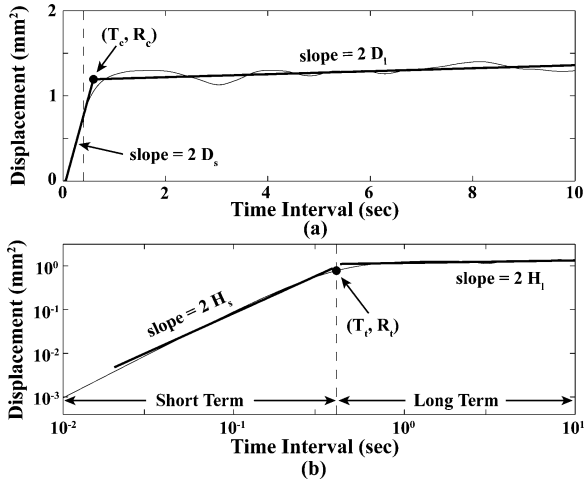

Fig. 3. SDF as a function of time interval in (a) linear and (b) logarithmic domains, showing the parameters of interest. The vertical dashed line marks the transition time.

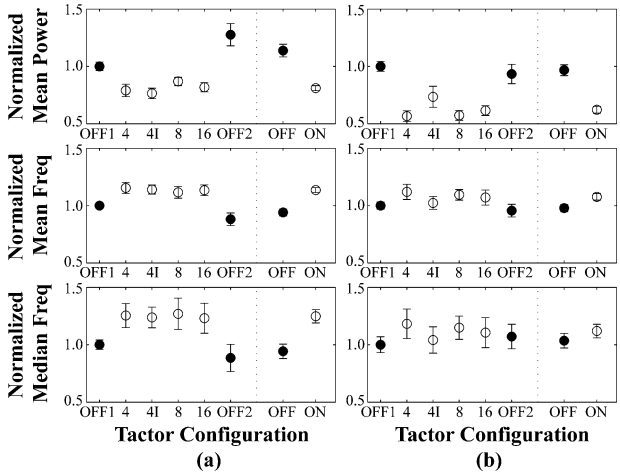

Fig. 4. Comparison of normalized mean spectral power, mean power frequency and median power frequency across tactor configurations for (a) M/L and (b) A/P tilt. The dotted line separates the results for individual tactor configurations from the combined tactors OFF and ON configurations. Error bars indicate standard error of the mean.

V. Results

A. PSD Analysis

PSD analysis provides the spectral distribution of the trunk tilt in the A/P and the M/L directions. Vibrotactile feedback produced consistent decreases in mean spectral power and increases in mean and median frequencies for each tactor configuration compared to OFF1, for both A/P and M/L tilts, with many of these differences being significant (see Fig. 4). Significance was defined at the $p < 0.05$ level. There were no significant differences among the four tactor configurations, except for a slightly higher average A/P power for 4I.

The power spectra were compared across tactor configurations and no significant differences were found. The trials were combined into "tactors OFF" and "tactors ON" groups, showing reductions in average spectral power of 38% ($p < 0.00001$) and 29% ($p < 0.0001$) with tactors ON in the A/P and M/L directions,

TABLE I
PSD PARAMETERS FOR A/P AND M/L TILTS. MEAN ± STANDARD ERROR OF MEAN SHOWN FOR TACTORS OFF (48 CYCLES), TACTORS ON (96 CYCLES), AND PERCENTAGE CHANGE

	Tactors OFF	Tactors ON	% Change	Significance
Mean spectral power (x1000 deg^2/Hz)				
A/P	168 ± 19	97 ± 5	-35.6 ± 3.1	$p < 0.00001$
M/L	28.2 ± 2.4	19.8 ± 0.9	-28.8 ± 1.9	$p < 0.00001$
Mean power frequency (Hz)				
A/P	0.352 ± 0.015	0.383 ± 0.011	+10.1 ± 3.0	$p < 0.002$
M/L	0.398 ± 0.019	0.473 ± 0.012	+20.7 ± 2.4	$p < 0.00001$
Median power frequency (Hz)				
A/P	0.258 ± 0.015	0.271 ± 0.012	+8.1 ± 5.7	N/S
M/L	0.301 ± 0.020	0.377 ± 0.012	+32.4 ± 6.1	$p < 0.00001$

The significance level of the percentage change is given (N/S = not significant at $p < 0.05$).

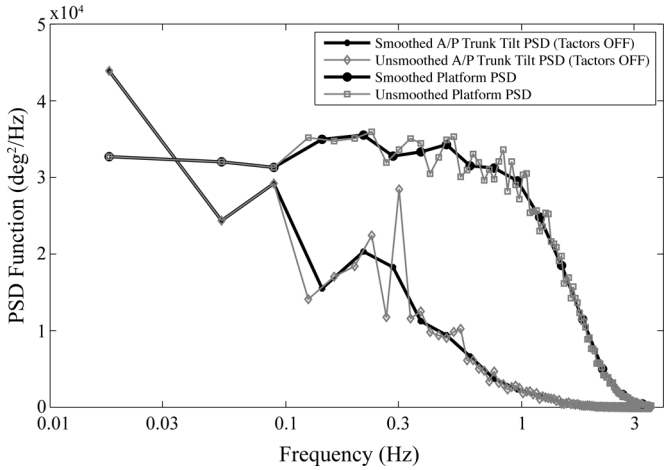

Fig. 5. Comparison of smoothed and unsmoothed PSD functions for platform stimulus and A/P tilt (Tactors OFF configuration).

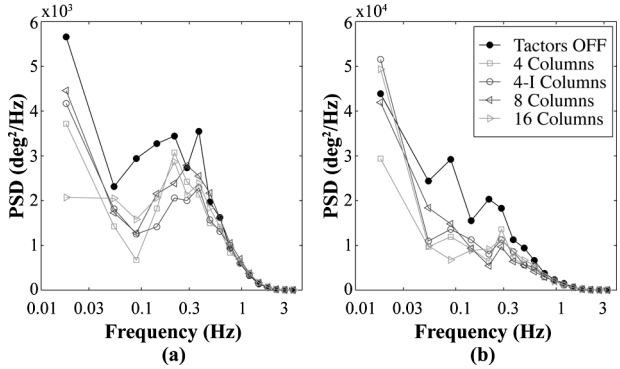

Fig. 6. (a) PSD plot of M/L trunk tilt for all tactor configurations. (b) PSD plot of A/P trunk tilt for all tactor configurations and platform stimulus.

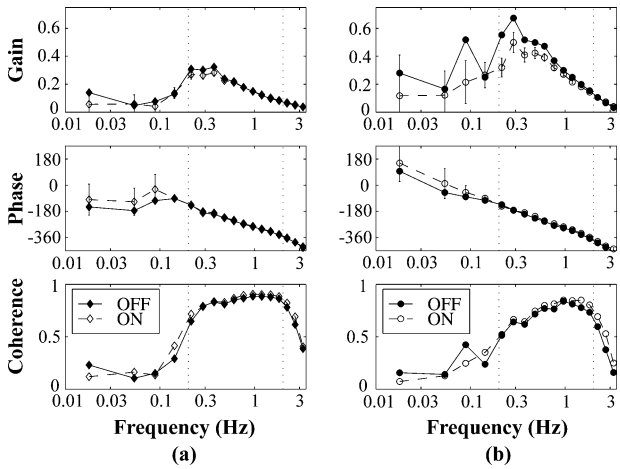

Fig. 7. Mean gain, phase, and coherence function estimate for eight subjects in (a) M/L and (b) A/P directions. Dotted lines mark the frequency range (0.2–2.0 Hz) in which consistent differences were typically found.

respectively (see Table I). Mean power frequency increased by 10% ($p < 0.003$) in the A/P direction and 21% ($p < 0.00001$) in the M/L direction. Median frequency increased by 8% in the A/P (not significant) direction and 32% in the M/L ($p < 0.0001$) direction.

The PSDs of the platform stimulus and the A/P and M/L trunk tilts were smoothed into 17 frequency bins (see Fig. 5). Averaging across subjects for each tactor configuration showed that tilt power was reduced to a greater extent at lower frequencies than at higher frequencies for each of the tactors ON conditions, and there was no consistent difference observed among these four configurations (see Fig. 6). All further analyses combined the tactor configurations and compared responses with tactors ON to OFF conditions.

B. Transfer Function Analysis

Transfer functions were computed with platform velocities along y and x directions as the stimuli (inputs) and trunk tilt in A/P and M/L directions as the responses (outputs). Platform velocity was chosen as the stimulus input because the platform linear velocity command was generated using the PRPS. Trunk tilt, which the subject was instructed to control, was selected as the output. Fig. 7 shows the mean gain, phase and coherence function estimate averaged across all subjects in the tactors OFF and ON conditions; error bars denote 95% confidence intervals of the mean. The gain of the transfer function indicates the extent of trunk tilt in response to the translational velocity of the platform at a particular frequency, a value of 1 implying trunk tilt amplitude of 1° for translational motion amplitude of 1 mm/s at a particular frequency. As observed in Fig. 7, there is a reduction in the gain in the tactors ON condition in comparison to tactors OFF condition.

The ratio of the mean gain for tactors ON to tactors OFF quantifies the extent to which the vibrotactile feedback was effective across different frequency bins (see Fig. 8). Statistically significant gain reduction (gain ratio less than 1) was observed at frequencies ranging from 0.2 to 2 Hz for all tactor configurations in the A/P direction and from 0.2 to 0.6 Hz in the M/L direction. Also, there was a gain ratio greater than 1 for frequencies greater than 2.0 Hz in the A/P and the M/L directions. However, the spectral power content associated with trunk tilt is very low at these frequencies. The degree of gain reduction was greater in A/P than in M/L, since the A/P direction is inherently less stable in stance, and therefore, provides more room for improvement. Phase was significantly increased for frequencies greater than 0.3 Hz, suggesting an improved reaction time.

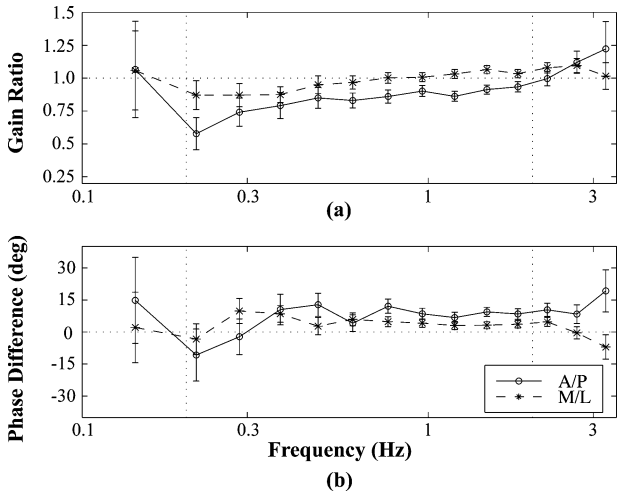

Fig. 8. (a) Gain ratio and (b) phase difference plotted for the tactors OFF and tactors ON conditions for A/P and M/L tilt directions.

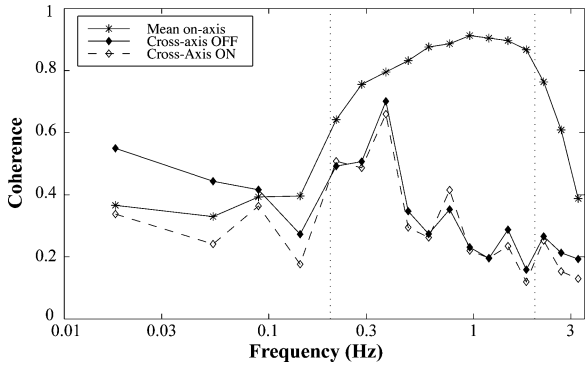

Fig. 9. Coherence function for the mean of same axis, cross-axis coherence functions for the means of tactors ON and OFF conditions.

Coherence was consistently high in the frequency range from 0.2 to 2.0 Hz (see Fig. 7), thus indicating a high correlation between the stimulus and response in both the A/P and M/L directions, regardless of whether the tactors were ON or OFF. Statistically significant changes in the gain were also observed in this range. Gain was reduced, to a greater extent, at lower frequencies (<0.2 Hz), but this was not significant due to the low coherence values. The average of these coherence functions contrasts with the cross-axis coherence function plot (stimulus as x-direction platform velocity and response as A/P trunk tilt) for tactors ON and OFF (see Fig. 9). This low cross-axis correlation suggests that there is not a strong linear coupling of postural control strategy in the A/P and M/L directions.

C. SDA Results

Mean SDFs are shown for a typical subject with tactors OFF and ON, in each of the A/P and M/L directions, with circles marking the transition points (see Fig. 10). The planar SDF is not shown because it is simply the sum of the A/P and M/L curves. The mean-square displacement is lower for M/L than for A/P, which is indicative of the improved stability in that

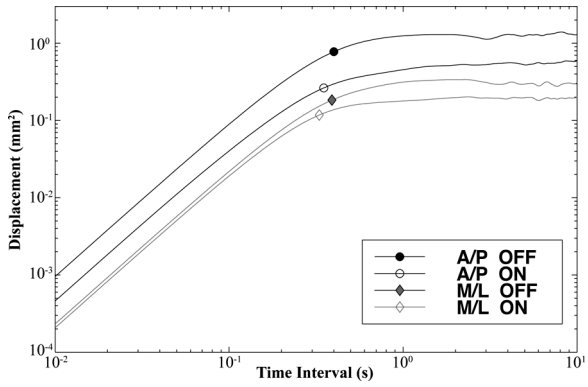

Fig. 10. SDFs and associated transition points for A/P and M/L tilts, with and without tactors, for a single subject.

TABLE II
STABILOGRAM DIFFUSION PARAMETERS FOR A/P, M/L, AND PLANAR TILTS

	Tactors OFF	Tactors ON	% Change	Significance
Scaling exponent (H_s)				
A/P	0.842 ± 0.013	0.859 ± 0.005	+2.2 ± 1.2	N/S
M/L	0.863 ± 0.007	0.870 ± 0.005	+0.7 ± 0.4	N/S
Planar	0.845 ± 0.010	0.862 ± 0.004	+2.1 ± 0.9	trend
Transition time (T_t)				
A/P	0.586 ± 0.079	0.461 ± 0.036	-17.6 ± 5.0	p < 0.01
M/L	0.481 ± 0.041	0.436 ± 0.040	-9.2 ± 3.1	p < 0.05
Planar	0.566 ± 0.067	0.450 ± 0.033	-17.5 ± 4.7	p < 0.01
Transition displacement (R_t)				
A/P	1.576 ± 0.430	0.786 ± 0.139	-43.5 ± 8.7	p < 0.01
M/L	0.221 ± 0.036	0.176 ± 0.027	-15.2 ± 7.6	trend
Planar	1.800 ± 0.439	0.961 ± 0.148	-40.9 ± 7.8	p < 0.01
Diffusion coefficient (D_s)				
A/P	1.652 ± 0.483	0.980 ± 0.176	-31.5 ± 7.9	p < 0.01
M/L	0.259 ± 0.037	0.229 ± 0.031	-7.0 ± 6.7	N/S
Planar	1.912 ± 0.497	1.220 ± 0.186	-28.5 ± 6.8	p < 0.01
Critical time (T_c)				
A/P	0.956 ± 0.117	0.793 ± 0.062	-14.3 ± 4.1	p < 0.01
M/L	0.852 ± 0.098	0.703 ± 0.068	-15.8 ± 4.6	p < 0.02
Planar	0.932 ± 0.096	0.773 ± 0.058	-15.5 ± 3.0	p < 0.01
Critical displacement (R_c)				
A/P	2.799 ± 0.874	1.398 ± 0.230	-41.7 ± 7.5	p < 0.001
M/L	0.417 ± 0.088	0.298 ± 0.043	-22.2 ± 7.0	p < 0.02
Planar	3.245 ± 0.935	1.708 ± 0.246	-39.6 ± 6.7	p < 0.001

Mean ± standard error of the mean is shown for tactors OFF, tactors ON, and percentage change with tactors, averaged across eight subjects. The significance level of the percentage change is given (N/S = not significant at $p < 0.05$).

direction. Vibrotactile feedback reduces the displacement across all time intervals, proportionately more in A/P than M/L, and decreases the transition time. The long-term region is quite flat, resulting in very low values for D_l and H_l (typically <0.05 and 0.1, respectively). No significant or consistent differences were seen in either parameter.

Population mean and standard error of the mean are summarized for the other six parameters (see Table II). Tactor effects were tested for each parameter by calculating the percentage change from tactors OFF to tactors ON condition. Significant decreases were seen in both transition and critical time, and displacement for A/P, M/L, and planar data; the sole exception is the M/L transition displacement, which showed a trend toward significance (defined as $p < 0.1$ and at least seven of eight subjects showing a change in the same direction).

The reduction in the short-term diffusion coefficient D_s was significant for A/P and planar tilt data, but not for M/L. The short-term scaling exponent H_s was slightly increased with tactors ON for seven subjects, but it was slightly decreased for one subject, which prevented the difference from becoming significant.

Generally, parametric changes in the A/P direction were also apparent in M/L, but to a lesser extent. The combination resulted in planar tilt changes that were similar in magnitude to A/P, but statistically more significant. The coefficient of variation (ratio of standard error to mean) of the A/P parameters was reduced by about 40% with tactors ON. This may be partially due to the larger number of cycles for tactors ON, but it is comparable to the difference between A/P and M/L with tactors OFF.

VI. Discussion

This study provides information about the frequency-dependent reductions in body sway measures (trunk tilts) and the corresponding reductions in stabilogram diffusion parameters, which furthers our understanding of the effect of the vibrotactile balance aid on human postural control during multidirectional perturbations. Since the study was performed on subjects with vestibular deficits who had no visual cues (eyes closed), the subjects relied on their native compromised vestibular cues and proprioceptive cues along with the information provided by the vibrotactile feedback balance aid. The reduction in gains of the frequency transfer functions computed for body sway responses in the A/P and the M/L directions suggests that the vibrotactile feedback improves the sensitivity of the human postural control system to external platform disturbances since lower gain values imply lower body trunk tilts. This is achieved by augmenting native inputs with the cues provided by the vibrotactile feedback.

The stimulus and the body sway responses were analyzed in the frequency domain to calculate parameters such as average spectral power, median and mean power frequencies, transfer function gain, phase, and coherence. The reduction in the average spectral power with vibrotactile feedback is consistent with the findings in the time domain that the RMS body sway is reduced with vibrotactile feedback [7].

The increase in the median and mean power frequencies for the A/P and M/L body sway suggest that the reduction of the spectral power is not uniform across all the frequencies and the reduction in higher frequencies is less than that at lower frequencies. Therefore, more detailed PSD functions were computed. PSDs of the body sway tilt indicate that the spectral power reduction at higher frequencies is less than the reduction at lower frequencies and the reduction is not significant beyond a certain cutoff frequency. A recent paper by Goodworth *et al.* [22] systematically varied the vibrotactile feedback parameters, while healthy subjects were given pseudorandom pitch inputs. That paper showed a pattern in the phase of the frequency response (similar to what we report here) that could be explained by the integral nature of the vibrotactile feedback device, and also concluded that in persons without vestibulopathies, the vibrotactile feedback could be considered as providing an augmented input, as contrasted to a "sensory reweighting" process. Whether it is possible to extrapolate to the performance of vestibulopathic subjects from those having normal vestibular function merits further investigation.

Transfer function analysis in the frequency domain provided information not only about the gain variation across the various frequencies, but also about the phase changes. The reduction in gain is consistent with the findings of the PSD analysis. The reduction in phase lag implies that the time delay associated with postural correction was decreased with vibrotactile feedback. However, the gain and phase data at higher frequencies suggest that the improved phase lag is insufficient to make corrections in posture at those frequencies, and therefore, there is no considerable gain reduction. The low cross-axis correlation suggests that postural control strategy in the A/P and M/L directions are not strongly coupled.

SDA results suggest that subjects were able to sense the vibrotactile information and generate a postural correction more quickly, as evidenced by the increased phase and decreased critical time, resulting in improved closed-loop postural control at frequencies below 2 Hz. The decreased critical time suggests that the onset of closed-loop control over open-loop control occurs earlier with vibrotactile feedback than with no feedback. The reduced critical displacement and short-term diffusion coefficient, which quantifies stochastic activity, demonstrate improvements to the accuracy and repeatability of the open-loop control system as well. Maurer and Peterka [23], [24] have proposed a model with a proportional, integral, and derivative (PID) controller to explain the experimentally observed changes in the SDFs, eliminating the need for true open-loop postural control. In terms of this closed-loop model, the reductions in critical time and displacement could be largely explained by increases in the proportional and derivative gains, but the reduction in the diffusion coefficient also suggests a decrease in the time delay. The sensory feedback provided by the balance aid consists of proportional and derivative information regarding body tilt, which would be more rigorously modeled in the feedback path rather than by the neural controller in the forward path. While it is unclear whether the open-loop region has a physiological basis, the SDA and PID techniques both appear suitable for quantifying the effects of the balance aid.

All of the analytical techniques showed reduced variability with the addition of vibrotactile feedback. It implies that there is tighter regulatory control with vibrotactile feedback, thereby reducing the stochastic activity of the body sway. The shortened latency of postural corrections results in a slight increase in the short-term scaling exponent and the transfer function gain above 2.5 Hz, but this is more than offset by the large reductions in sway at low to midrange frequencies. These improvements are seen in both A/P and, to a lesser extent, in M/L directions.

Postural sway improvements have been effected during quiet stance using subthreshold white noise vibrations, resulting in reductions of 5%–20% in the critical displacement and long-term scaling exponent and diffusion coefficient [25], [26]. However, no changes to the critical time or short-term diffusion coefficients were reported, and the change in displacement falls short

of the 40% seen herein, supporting the need for suprathreshold coordinated vibrotactile feedback.

Moreover, the lack of consistent differences in the PSD plots of the body sway for different tactor configurations suggests that the spatial resolution of the tactors does not affect subjects' performance in terms of either improved sway reduction or in frequency bandwidth. It has been previously shown that the central nervous system controls the recovery from multiple direction perturbations by decoupling the postural space into two orthogonal directions (A/P and M/L) [12]. The lack of any significant differences in performance based on display configuration provides strong evidence that the four-column display is optimal from the standpoint of reduced device design complexity for applications of multidirectional perturbed stance. The low cross-axis coherence values justified the evaluation of the 4I tactor configuration (independent A/P and M/L feedback).

Van Erp [27] showed that using the midaxis as the origin in a tactile torso display results in a systematic bias between the tactor direction and the experienced direction (bias toward the midsagittal plane). Cholewiak *et al.* [28] demonstrated that anatomically defined anchor points provide localization referents (such as the navel and spine) that enhance performance even with wide target spacing. Furthermore, they determined that spatial accuracy is affected by the selection of such anchor points for a vibrotactile torso display; near optimal performance was found at the navel and spine. Based on the results of both the time-domain analysis described in [7] and the frequency-domain analysis described herein, the findings do not suggest that humans gainfully benefit from a vibrotactile display with a spatial resolution greater than 90°. Therefore, with respect to the other sensory substitution technology currently being explored (i.e., electrotactile and auditory), the electrotactile feedback system known as BrainPort that provides a 10×10 electrode array [29] may be superfluous for real-time standing applications. Furthermore, in addition to the suggestion that only four columns are required to aptly describe tilt direction, the results from [7] suggest that only three states (OFF and tactor rows one and two) are sufficient for coding tilt magnitude (versus four states: OFF and ON rows 1–3). These data should be taken into account in future device design iterations.

ACKNOWLEDGMENT

The authors would like to thank J. Robertsson, H. Kubert, Dr. K. Statler, and M. Christensen for their help in data collection, Dr. L. Oddsson for his contribution to the experimental design and for the use of his research facilities, and Dr. M. Weinberg for his input regarding data analysis.

REFERENCES

[1] L. M. Nashner, F. O. Black, and C. Wall, 3rd, "Adaptation to altered support and visual conditions during stance: Patients with vestibular deficits," *J. Neurosci.*, vol. 2, pp. 536–544, 1982.

[2] P. Bach-y-Rita, "Tactile sensory substitution studies," *Ann. New York Acad. Sci.*, vol. 1013, pp. 83–91, 2004.

[3] M. Dozza, L. Chiari, and F. B. Horak, "Audio-biofeedback improves balance in patients with bilateral vestibular loss," *Arch. Phys. Med. Rehabil.*, vol. 86, pp. 1401–1403, 2005.

[4] J. Hegeman, "The balance control of bilateral peripheral vestibular loss subjects and its improvement with auditory prosthetic feedback," *J. Vestib. Res.*, vol. 15, pp. 109–117, 2005.

[5] E. Kentala, J. Vivas, and C. Wall, III, "Reduction of postural sway by use of a vibrotactile balance prosthesis prototype in subjects with vestibular deficits," *Ann. Otol. Rhinol. Laryngol.*, vol. 112, pp. 404–409, 2003.

[6] C. Wall, 3rd and E. Kentala, "Control of sway using vibrotactile feedback of body tilt in patients with moderate and severe postural control deficits," *J. Vestib. Res.*, vol. 15, pp. 313–325, 2005.

[7] K. H. Sienko, M. D. Balkwill, L. I. E. Oddsson, and C. Wall, 3rd, "Effects of multi-directional vibrotactile feedback on postural performance during continuous multi-directional support surface perturbations," *J. Vestib. Res.*, vol. 18, pp. 273–285, 2008.

[8] R. Johansson, M. Magnusson, and M. Akesson, "Identification of human postural dynamics," *IEEE Trans. Biomed. Eng.*, vol. 35, no. 10, pp. 858–69, Oct. 1988.

[9] D. A. Winter, A. E. Patla, F. Prince, M. Ishac, and K. Gielo-Perczak, "Stiffness control of balance in quiet standing," *J. Neurophysiol.*, vol. 80, pp. 1211–1221, 1998.

[10] J. Jeka, K. S. Oie, and T. Kiemel, "Multisensory information for human postural control: Integrating touch and vision," *Exp. Brain Res.*, vol. 134, pp. 107–125, 2000.

[11] T. Mergner and T. Rosemeier, "Interaction of vestibular, somatosensory and visual signals for postural control and motion perception under terrestrial and microgravity conditions: a conceptual model," *Brain Res. Rev.*, vol. 28, pp. 118–135, 1998.

[12] Z. Matjacic, M. Voigt, D. Popovic, and T. Sinkjaer, "Functional postural responses after perturbations in multiple directions in a standing man: A principle of decoupled control," *J. Biomech.*, vol. 34, pp. 187–196, 2001.

[13] M. C. K. Khoo, "Physiological Controls Systems," in *IEEE Press Series in Biomedical Engineering*, M. Akay, Ed. New York: Wiley, 2000.

[14] J. S. Bendat and A. G. Piersol, *Random Data: Analysis and Measurement Procedures*. New York: Wiley, 2000.

[15] R. K. Otnes and L. Enochson, *Digital Time Series Analysis*. New York: Wiley, 1972.

[16] R. J. Peterka and C. Wall, 3rd, "Determining the effectiveness of a vibrotactile balance prosthesis," *J. Vestib. Res.*, vol. 16, pp. 45–56, 2006.

[17] V. V. Vichare, C. Wall, III, M. D. Balkwill, and K. H. Sienko, "Assessing the effect of vibrotactile feedback during continuous multidirectional platform motion: A frequency domain approach," in *Proc. 31st Annu. Int. Conf. IEEE Eng. Med. Biol.*, Minneapolis, MN, 2009, pp. 6910–6913.

[18] J. J. Collins and C. J. D. Luca, "Open-loop and closed-loop control of posture: A random-walk analysis of center-of-pressure trajectories," *Exp. Brain Res.*, vol. 95, pp. 308–318, 1993.

[19] L. I. Oddsson, C. Wall, 3rd, M. D. McPartland, D. E. Krebs, and C. A. Tucker, "Recovery from perturbations during paced walking," *Gait Posture*, vol. 19, pp. 24–34, 2004.

[20] G. E. P. Box, W. G. Hunter, and J. S. Hunter, *Statistics for Experimenters: An Introduction to Design, Data Analysis, and Model Building*. New York: Wiley, 1978.

[21] R. J. Peterka, "Sensorimotor integration in human postural control," *J. Neurophysiol.*, vol. 88, pp. 1097–1118, 2002.

[22] A. D. Goodworth, C. Wall, and R. J. Peterka, "Influence of feedback parameters on performance of a vibrotactile balance prosthesis," *IEEE Trans. Neural Syst. Rehabil. Eng.: Publ. IEEE Eng. Med. Biol. Soc.*, vol. 17, pp. 397–408, 2009.

[23] C. Maurer and R. J. Peterka, "A new interpretation of spontaneous sway measures based on a simple model of human postural control," *J. Neurophysiol.*, vol. 93, pp. 189–200, 2005.

[24] R. J. Peterka, "Postural control model interpretation of stabilogram diffusion analysis," *Biol. Cybern.*, vol. 82, pp. 335–343, 2000.

[25] A. Priplata, J. Niemi, M. Salen, J. Harry, L. A. Lipsitz, and J. J. Collins, "Noise-enhanced human balance control," *Physical Review Letters*, vol. 89, pp. 238101-1–238101-4, 2002.

[26] A. Priplata, J. Niemi, J. Harry, L. A. Lipsitz, and J. J. Collins, "Vibrating insoles and balance control in elderly people," *Lancet*, vol. 362, pp. 1123–1124, 2003.

[27] J. B. F. V. Erp, "Presenting directions with a vibrotactile torso display," *Ergonomics*, vol. 48, pp. 302–313, Feb. 2005.

[28] R. W. Cholewiak, J. C. Brill, and A. Schwab, "Vibrotactile localization on the abdomen: Effects of place and space," *Percept. Psychophys.*, vol. 66, pp. 970–987, 2004.

[29] Y. P. Davilov, M. E. Tyler, K. L. Skinner, R. A. Hogle, and P. Bach-y-Rita, "Efficacy of electrotactile vestibular substitution in patients with peripheral and central vestibular loss," *J. Vestib. Res.*, vol. 17, pp. 119–130, 2007.

Kathleen H. Sienko received the B.S. degree in materials engineering from the University of Kentucky, Lexington, in 1998, the S.M. degree in aeronautics and astronautics from Massachusetts Institute of Technology (MIT), Cambridge, in 2000, and the Ph.D. degree in medical engineering and bioastronautics from the Harvard-MIT Division of Health Sciences and Technology, Cambridge, in 2007.

She was a Research Engineer with the Massachusetts Eye and Ear Infirmary, Harvard Medical School, Boston, MA. She is currently an Assistant Professor in mechanical and biomedical engineering with the University of Michigan, Ann Arbor, where she is also the Director of the Sensory Augmentation and Rehabilitation Laboratory.

Prof. Sienko is a member of American Society of Mechanical Engineers and American Society for Engineering Education.

Vivek V. Vichare received the B.Tech. and M.Tech degrees in mechanical engineering from the Indian Institute of Technology, Bombay, India.

He is currently with the Sensory Augmentation and Rehabilitation Laboratory, Department of Mechanical Engineering, University of Michigan, Ann Arbor.

M. David Balkwill received the B.Math degree in applied math and computer science from the University of Waterloo, Waterloo, Canada, and the S.M. degree in aeronautics and astronautics from Massachusetts Institute of Technology, Cambridge.

He is currently a Biomedical Project Engineer with the Jenks Vestibular Diagnostic Laboratory, Massachusetts Eye and Ear Infirmary, Harvard Medical School, Boston.

Conrad Wall, III (M'75) received the B.S. and M.S. degrees in physics from Tulane University, New Orelans, LA, and the Ph.D. degree in bioengineering from Carnegie Mellon University, Pittsburgh, PA.

He is currently a Professor of otology and laryngology with Harvard Medical School, Boston, MA, where he is also the Founder and the Director of the Jenks Vestibular Diagnostic Laboratory, Massachusetts Eye and Ear Infirmary and participated in sponsored research and in the joint Harvard-Massachusetts Institute of Technology, Whitaker College of Health Sciences Technology, Cambridge. He is also a Project Leader and an Associate Team Leader in the Neurovestibular Adaptation Team of National Aeronautics and Space Administration's National Space Biomedical Research Institute, Houston, TX and a Project Leader of the balance project of the Infirmary's Neural Prosthesis Research Center. He chairs the working group in charge of the American National Standards Institute standard on the vestibular function test battery.

Dr. Wall is a Fellow in the American Institute for Medical and Biological Engineering.